Proceedings of the Tenth Pacific Conference on Earthquake Engineering
Building an Earthquake-Resilient Pacific
6-8 November 2015, Sydney, Australia

Simulation of 2D site response at Heathcote Valley during the 2010-2011 Canterbury earthquake sequence

S. Jeong & B. A. Bradley

University of Canterbury, Christchurch, New Zealand

ABSTRACT: The strong motion station at Heathcote Valley School (HVSC) recorded unusually high peak ground accelerations (2.21g vertical and 1.41g horizontal) during the February 2011 Christchurch earthquake. Ground motions recorded at HVSC in numerous other events also exhibited consistently higher intensities compared with nearby strong motion stations. This study investigates the characteristics of the valley dynamic response at HVSC by means of 2D dynamic finite element analyses, where recorded motions at LPCC (Lyttelton Port Company station) are used as input motions for the analyses. The simulation agrees well with the observation and suggests that the motions at HVSC are amplified in a wide band of frequencies. Simulations also suggest that Rayleigh waves, generated at the inclined interface of the surficial colluvium and underlying volcanic rock, strongly affect the ground motions recorded at HVSC. Sensitivity analyses demonstrate the importance of proper site characterization for a successful prediction of the site response.

1 INTRODUCTION

Numerous intense ground motions were recorded during the 22 February 2011 Christchurch earthquake. Peak ground acceleration recorded at Heathcote Valley School station (HVSC) exceeded 2g in vertical component, and 1.4g in horizontal component (Bradley & Cubrinovski 2011). Other ground motions recorded at HVSC during the 2010-2011 Canterbury earthquake sequence also exhibited consistently higher intensities compared with nearby strong motion stations (Bradley 2012; Bradley 2013). Figure 1 provides a comparison of ground motions recorded at Heathcote Valley School station (HVSC) and the nearby Lyttelton Port Company station (LPCC) during the three largest shaking events of the earthquake sequence. The locations of these two stations are shown in Figure 2.

HVSC is located close to the edge of Heathcote valley, where shallow, firm colluvium sediments mantle weathered volcanic rock. Heathcote valley is a V-shaped valley facing north, surrounded by the volcanic Port Hills. Fine silts (loess)—originating from glacial and river erosion of the Southern Alps during the cold cycles of the Quaternary—are predominant in surficial soils in the Port Hills area, which were deposited by Aeolian process and then washed down to the valley along with volcanic rock debris to form the colluvium (Brown *et al.* 1992). The thickness of surficial soil varies from a few metres on the ridges to 20-30 metres in the valleys.

Various studies (Bradley 2012; Bradley 2013; Gelagoti *et al*. 2014) have suggested that the wave interference caused by the complex subsurface valley geometry could have been a major contribution to the intensity of ground motions recorded at HVSC. Based on an empirical analysis using 10 most significant events, Bradley (2013) showed that HVSC exhibits systematic site amplification at $f > 2$ Hz. Gelagoti *et al*. (2014) performed preliminary 2D site response simulations of Heathcote Valley based on various assumptions on the dynamic soil properties and valley geometries and suggested that the strongly inelastic soil behaviour, combined with 2D/3D valley geometry, may explain the high amplitude of shaking.

This paper presents a case study of site amplification effects at Heathcote Valley via observations and numerical simulations. A summary of the geophysical site characterization is first presented, followed by presentation of the salient results from a series of 2D site response analyses to investigate the effects of the valley stratigraphy, surface topography, and the soil-bedrock impedance contrast on the simulated intensity of ground shaking at HVSC as compared to observations.

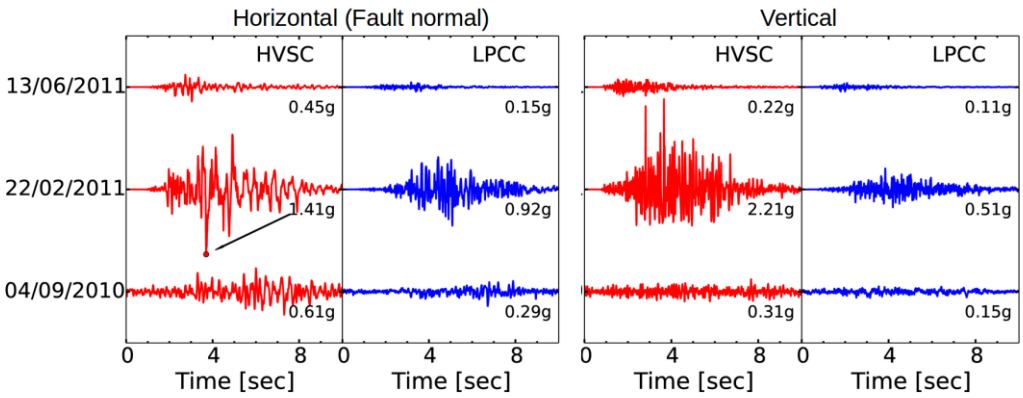

Figure 1. Comparison of horizontal (fault normal component) and vertical acceleration time histories recorded at HVSC and LPCC over the three largest shaking events in the Canterbury earthquake sequence (all acceleration amplitudes to scale with maximum values shown).

2 SITE CHARACTERIZATION

Fifteen seismic cone penetration test (sCPT) and five multi-channel analyses of surface waves (MASW) surveys were performed at Heathcote valley, the locations of which are plotted in Figure 2. The soundings were continued until refusal, at which the tip resistance (q_c) usually exceeded 40 MPa, indicative of volcanic rock. The sCPT results, summarized in Figure 3a, suggest that V_S is strongly depth dependent, a typical characteristic of non-plastic granular materials. This depth dependence is modelled by a power law equation as shown in Figure 3a:

$$V_S = 144\, z^{0.39} \tag{1}$$

A simplified two layer version of the velocity profile at HVSC is also shown in Figure 3a; the effect of such simplification will be discussed later in this paper. Seismic refraction and MASW surveys (Park *et al.* 1999) were performed using 24 horizontal and 24 vertical geophones and a 5 kg sledge hammer. Rayleigh and Love wave dispersion curves were obtained from the experimental data using a frequency domain beamforming technique (Johnson & Dudgeon 1992), and Geopsy (Wathelet 2005) was used for multi-modal inversion of the dispersion curves to obtain velocity profiles. The thickness of sediments obtained from CPT refusal depths, corroborated by MASW test result was spatially interpolated using the ordinary Kriging algorithm (Matheron 1963) to estimate the depth of the weathered rock over the region of interest, which underlies the surficial sediments. Figure 3b shows a contour plot of sediment depth, in which subaxes on the top and to the left of the main plot show cross sections of the valley with filled contours of shear wave velocity, approximated by Equation 1.

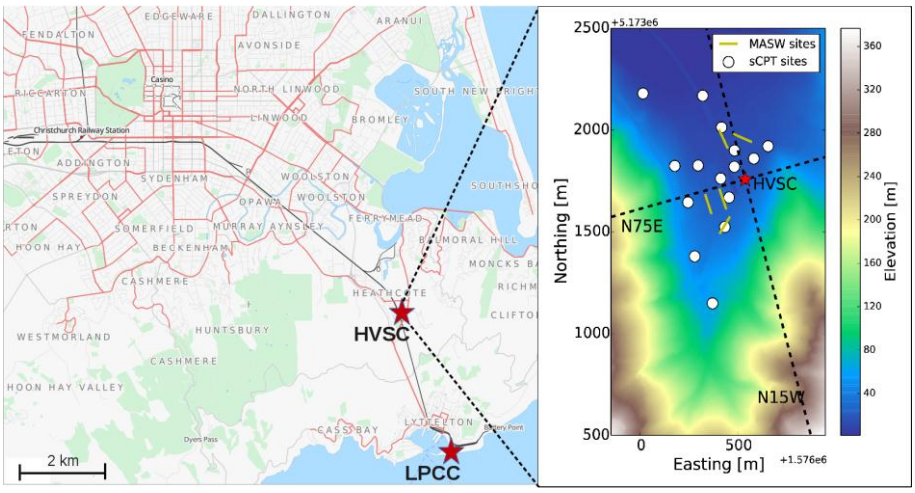

Figure 2. Location and topography of Heathcote valley, strong motion stations, and test sites.

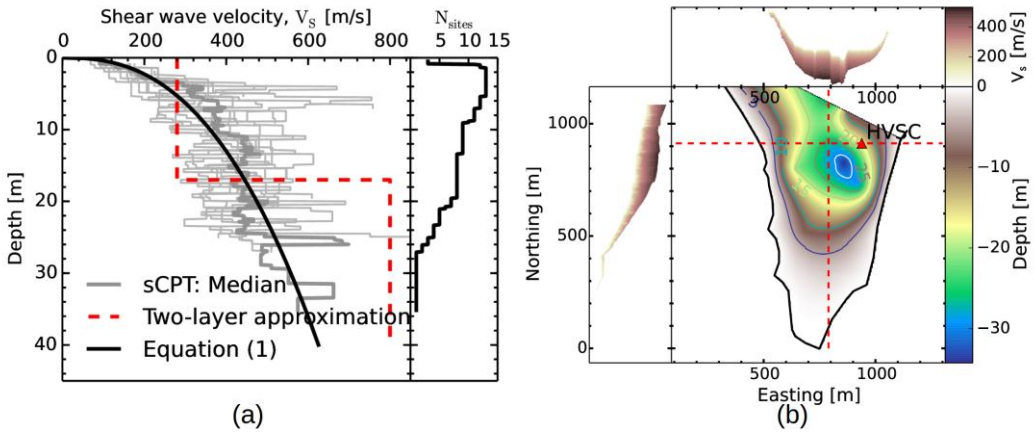

Figure 3. (a) Shear wave velocity of the loess colluvium at 15 locations in Heathcote valley as function of depth; (b) a contour plot of sediment depth obtained by spatial interpolation of sCPT and MASW data. Subaxes on top and on the left of the main plot show valley cross sections along the red dashed lines, with contours of shear wave velocity approximated by Equation 1.

3 MODEL DESCRIPTION

A series of 2D plane strain finite element analyses were performed using OpenSees (Mazzoni *et al.* 2007) for cross sections of the valley along the two different azimuths shown in Figure 2: N75E (across the valley) and N15W (down the valley). The two valley cross sections showed qualitatively similar responses, and therefore this paper focuses on the simulation of N75E cross section only. Figure 4 schematically illustrates the mesh geometry and boundary conditions of the numerical model. Lateral boundaries are treated with free-field boundary conditions to minimize spurious reflections. The absorbing boundary at the bottom of the models is achieved via Lysmer dashpots (Kuhlemeyer & Lysmer 1973) which are expressed by Equation 2:

$$C_X = \rho V_S, \text{ and } C_Y = \rho V_P \quad (2)$$

where ρ is the mass density; V_S and V_P are the shear and compressional velocities; and C_X and C_Y are the horizontal and the vertical dashpot coefficients. Both the soil and the rock are modelled with linear-elastic Poisson solids, with mass densities: ρ_{Soil} = 1.8 Mg/m^3 for the soil and ρ_{Rock} = 2.4 Mg/m^3 for the rock. While it is evident that the linear elastic model would not be appropriate for strong events such as the February event, it is expected that this would be reasonable for many smaller events. A stiffness proportional damping is assumed with the critical damping ratio, ζ = 0.01 at the frequency, f = 16 Hz. The pressure dependent shear wave velocity of the soil is modelled by Equation 1. The shear wave velocity of the weathered rock beneath the soil is estimated from the result of MASW as V_S = 800 m/s (although sensitivity studies of the rock profile modelling are presented subsequently). The model assumes the shear wave velocity of the halfspace as V_{SB} = 1520 m/s, the same as the shear wave velocity of the bedrock at LPCC (Wood *et al*. 2011).

The model is subjected to 9 events recorded during the 2010-2011 Canterbury earthquake sequence which are summarized in Table 1. The acceleration time series recorded at LPCC were deconvolved from one dimensional site response, using the shear wave velocity profile by Wood *et al*. (2011), and used as vertically incident input motions prescribed at the base of model via equivalent nodal forces.

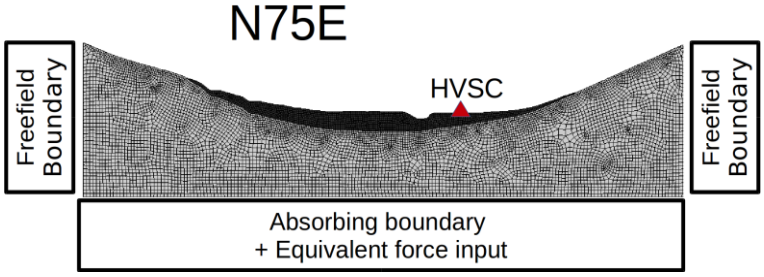

Figure 4. Two-dimensional mesh geometries and boundary conditions of the simulated valley cross section

Table 1. Earthquake events used in the analyses, in chronological order.

		HVSC			LPCC		
Event date	**M_W**	**R_{rup}* (km)**	**PGA** (g)**	**PGV** (cm/s)**	**R_{rup}* (km)**	**PGA** (g)**	**PGV** (cm/s)**
04/09/2010	7.1	20.8	0.61	29	22.4	0.29	19
19/10/2010	4.8	12.8	0.09	3.2	13.1	0.02	0.71
26/12/2010	4.7	4.7	0.11	2.9	7.7	0.02	0.65
22/02/2011	6.2	3.9	1.41	81	7	0.92	46
16/04/2011	5.0	7.3	0.68	32	5.2	0.29	8.5
13/06/2011 (a)	5.3	4.7	0.45	14	5.3	0.15	5.4
13/06/2011 (b)	6.0	3.6	0.91	55	5.8	0.64	33
21/06/2011	5.2	14.9	0.26	8.0	15.6	0.07	2.1
23/12/2011	5.9	9.7	0.26	42	12.4	0.44	23

*The shortest source-to-site distance based on Beavan *et al.* (2012); **Horizontal components

4 COMPARISON WITH RECORDED GROUND MOTIONS

Rather than directly comparing observed and simulated motions at HVSC, we herein compare the median HVSC/LPCC spectral ratio taken over all considered ground motions. LPCC is located on engineering bedrock with V_S = 1520 m/s, covered by only about 6 m of surficial soils with V_S = 300 m/s (Wood *et al.* 2011). The theoretical 1D transfer function at LPCC predicts negligible site effects at f < 7 Hz. An empirical study by Bradley (2013) also suggests that the site effect would be negligible at f < 5Hz. Therefore, HVSC/LPCC spectral ratios can be considered as a good approximation of the HVSC site response in f < 5 Hz, while it is also possible to obtain a better estimate of the HVSC site response by multiplying HVSC/LPCC spectral ratios by a theoretical transfer function of LPCC.

Figure 5 compares the simulated and recorded HVSC/LPCC spectral ratio, expressed principally via the median and ± std. values over all considered ground motions. Before computing the spectral ratios, the Fourier spectra are smoothed by the Konno & Ohmachi smoothing window (Konno and Ohmachi 1998) with the bandwidth parameter, b = 40. Overall, it can be seen that the comparison is satisfactory, and both the simulation and the observation suggest that ground motions at HVSC are amplified over a broad range of frequencies, for both the horizontal and vertical components. However, our numerical simulations under-predicted the horizontal component at f = 3 Hz and the vertical component for f = 6 Hz and > 10 Hz. The cause of this under-prediction is not yet clear, but it is expected that the limitations of the current model—relatively poor characterization of the dynamic properties of deeper rocks, and the contribution from out-of-plane waves that the model does not account for—would be partially responsible for this discrepancy.

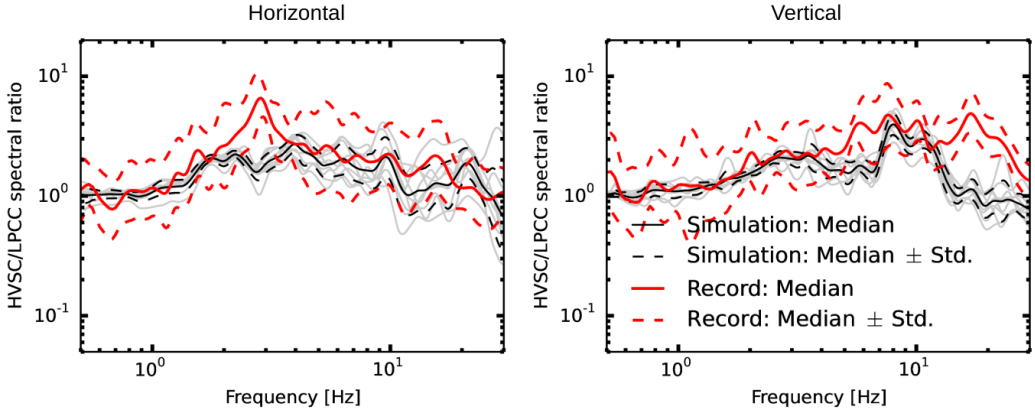

Figure 5. Simulated HVSC/LPCC spectral ratios compared with recorded spectral ratio. Individual simulations are shown in thin grey lines, and the median ± std. values are given for both the simulations and observations (the individual observed ratios are omitted for clarity).

5 AMPLIFICATIONS OF THE VERTICAL MOTIONS

Figure 6 compares the recorded and simulated vertical acceleration time series and Fourier spectra at HVSC for the 04/09/2010 event. The simulation was performed with both the horizontal and vertical input (plotted in black solid line), and compared with the simulation with only horizontal input (red dashed line). Simulated and recorded vertical accelerations compare very well for frequencies, $f < 10$ Hz, and the comparison of results with and without the vertical input motion reveals that mode-converted Rayleigh waves significantly contribute to the vertical response at f = 5-10 Hz or t > 15 sec. This finding is consistent throughout all considered events, and this suggests that the vertical motions observed at HVSC during the Canterbury earthquake sequence could have been strongly affected by the mode-converted Rayleigh waves—generated near the edge of the valley due to the basin geometry and strong impedance contrast—which propagates inwards along the valley surface.

However, it should be noted that the strong asymmetric vertical acceleration time series observed at various stations during the 22/02/2011 event (Fry *et al*. 2011) are often attributed to the combined effect of strong near-field shaking and non-linear response characteristics of near-surface granular materials (i.e. "Trampoline effect (Aoi *et al*. 2008)"). Such phenomenon obviously cannot be explained with the current model assumption of linear elastic soils. The role of non-linear soil response at HVSC during strong shaking is currently under investigation.

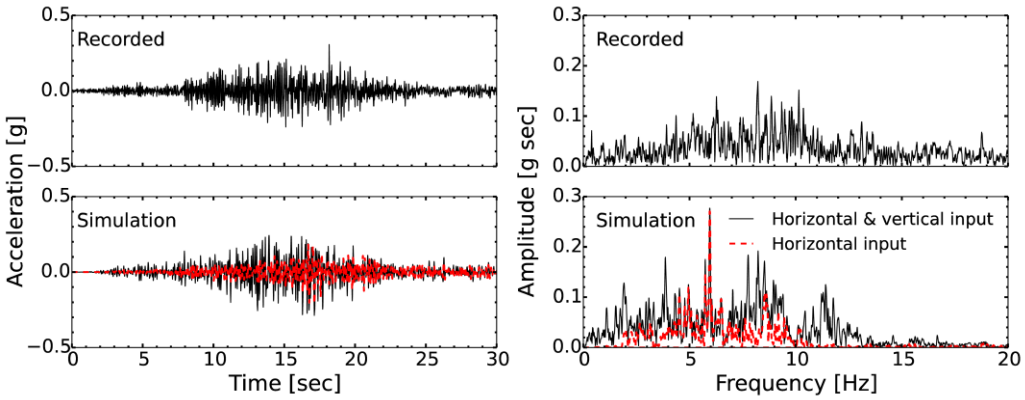

Figure 6. Comparison of recorded and simulated vertical acceleration time series and Fourier spectra at HVSC during the 04/09/2010 event: In the simulations, the black solid line shows the result with both horizontal and vertical input motion, whereas the red dashed line considered horizontal input only. Vertical accelerations at HVSC are strongly influenced by mode-converted Rayleigh waves at f = 5-10 Hz or t > 15 sec.

6 EFFECT OF VARIATIONS OF SHEAR WAVE VELOCITIES ON THE SITE RESPONSE AT HVSC

A parametric study was conducted to demonstrate the sensitivity of the valley site response to the modelled soil and rock V_S properties. Figure 7 shows the schematic diagram of the valley geometry, and Table 2 lists the velocity profiles considered in the parametric study. Profile 1 considers a common simplifying assumption of depth independent shear wave velocity of soils, whereas Profiles 2-4 considers possible scenarios of the rock velocity profile.

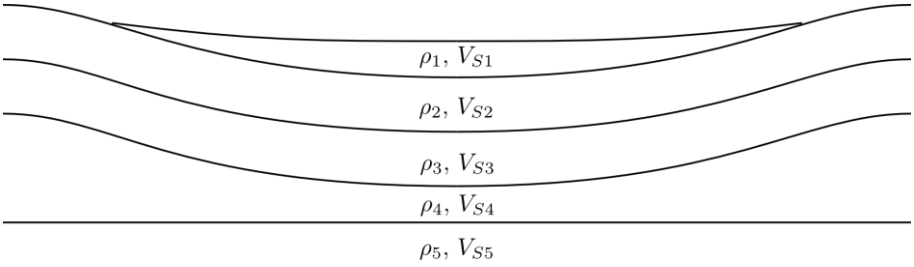

Figure 7. Schematic diagram showing the hypothetical rock velocity profiles

Table 2. List of velocity profiles considered in this study

	Profile 1	**Profile 2**	**Profile 3**	**Profile 4**
V_{S1} (m/s)	280	$144\ z^{0.39}$	$144\ z^{0.39}$	$144\ z^{0.39}$
V_{S2} (m/s)	800	800	800	800
V_{S3} (m/s)	800	800	800	1200
V_{S4} (m/s)	800	800	1500	1500
V_{S5} (m/s)	1500	1500	1500	1500

6.1 *Effect of the pressure dependent shear wave velocity of soils*

Figure 8 compares the HVSC/LPCC spectral ratios of Profiles 1 and 2, which describes the effect of the depth dependent shear wave velocity of soils. The response of the simplified two-layer model was overall comparable with the more realistic power law model (Equation 1). However, results also suggest that the simplified two-layer model overestimates the amplification of vertical motions near f = 7 Hz.

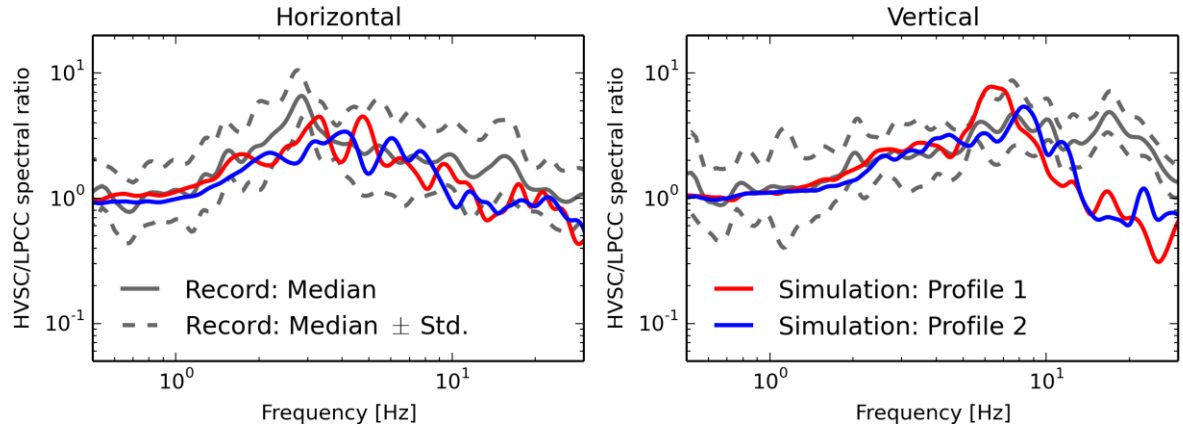

Figure 8. Effect of the pressure dependent shear wave velocity of the soil

6.2 *Effect of Rock velocity profiles*

The shear wave velocity of the weathered rock was estimated by means of MASW survey. However, our characterization of the rock shear wave velocity is quite poor, due to the practical limitations of MASW survey (i.e. the sledge hammer source has a shallow survey depth, and the passive source MASW requires a wide open space, flat surface topography, and a simple subsurface stratigraphy).

We therefore performed a sensitivity study, using 3 different velocity profiles for the weathered rock layers as described in Table 2 (Profiles 2-4), all of which are compatible with the result of geophysical site investigation. Figure 9 demonstrates the effect of rock shear wave velocity variations by comparing the HVSC/LPCC spectral ratios of Profiles 2, 3, and 4. The result shows that the response in high frequencies (i.e. f > 3 Hz for the horizontal component, and f > 6 Hz for the vertical component) is not sensitive to the choice of the rock velocity profile. The under-prediction of the valley response shown in Figure 5 more or less remained the same, regardless of the velocity profiles considered in this study. However, the response at lower frequencies was sensitive to the variation of the rock velocity profiles, even though the velocities of the shallowest (V_{S2}) and the deepest (V_{S5}) rock layers are kept constant and the geometry of valley layering is kept simple. The fact that none of considered rock profiles realistically model the observed horizontal peak at f = 3 Hz indicates that this is likely sensitive to the modelling of the soil layers, which will be further examined in future.

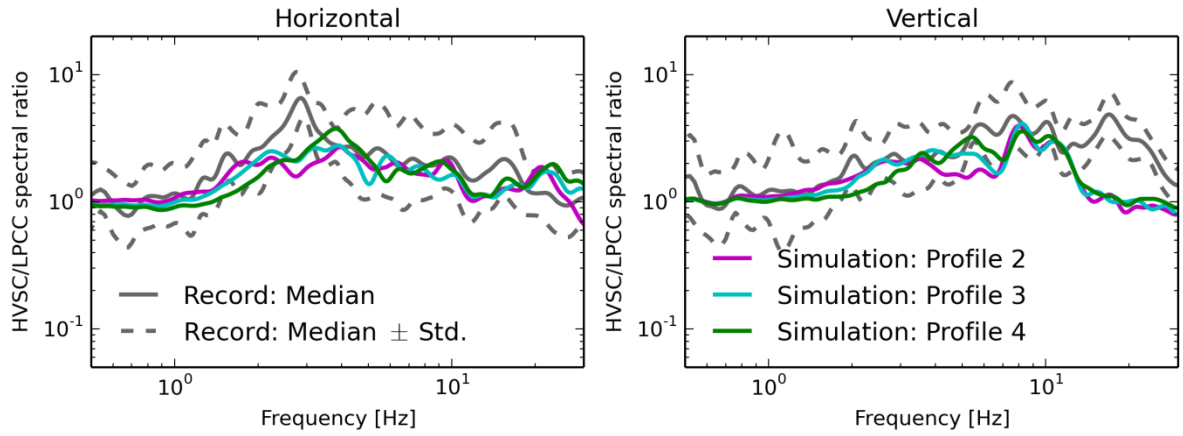

Figure 9. Effect of the rock velocity profile on the median HVSC/LPCC spectral ratios. The uncertainty in the simulated ratios across the considered events is relatively small and omitted for brevity.

7 CONCLUSIONS

This paper presents a case study on the site amplification effects at Heathcote Valley during the 2010-2011 Canterbury earthquake sequence through observations and 2D numerical simulations. An accurate 3D representation of the geological structure of Heathcote Valley was developed using a LiDAR-based DEM and in-situ geophysical test data obtained by sCPT and MASW. Based on the 3D representation of the geological structure, a series of 2D plane strain dynamic finite element simulations were undertaken, assuming that deconvolved motions recorded at LPCC can be used as the input motions at the base of the numerical model.

Both the observation and simulation show strong amplification over a wide range of frequencies in both the horizontal and vertical component. Comparisons of simulated and recorded ground motions demonstrate that the numerical model can simulate the recorded response of the valley at HVSC reasonably well, despite some inherent limitations.

The amplification of vertical motions is especially pronounced in higher frequencies. Comparisons of responses with and without vertical input motion suggests that vertical accelerations recorded at HVSC could have been strongly affected by basin-induced Rayleigh waves over a broad range of frequencies.

At Heathcote Valley, the site response at $f < 3$ Hz is largely dominated by the dynamic response of the rock layers, and at $f > 3$ Hz by the soil layers. This study has shown that employing a simplified homogeneous soil model overestimates the vertical response near $f = 7$ Hz, and that the velocities of rock layers needs to be accurately characterized if the low frequency ground motions are of importance.

8 ACKNOWLEDGEMENTS

Clinton M. Wood (University of Arkansas) kindly provided his MATLAB scripts for the beamforming analyses used in MASW surveys. Matthew Hughes (University of Canterbury) processed the DEM, which was used for modelling the surface topography. Financial support for this research was provided from the New Zealand Earthquake Commission (EQC) and Natural Hazards Research Platform.

REFERENCES:

Aoi S., Kunugi T., Fujiwara H. 2008. Trampoline effect in extreme ground motion., *Science*, **322**, 727-730.

Ashford, S.A., Sitar, N., Lysmer, J., & Deng, N. 1997. Topographic effects on the seismic response of steep slopes, Bull. Seismol. Soc. Am., **87**, 701–709.

Assimaki, D., & Jeong, S. 2013. Ground-Motion Observations at Hotel Montana during the M 7.0 2010 Haiti

Earthquake: Topography or Soil Amplification?, *Bull. Seismol. Soc. Am.*, **103**, 2577–2590.

Beavan, J., Motagh, M., Fielding, E. J., Donnelly, N., & Collett, D. 2012. Fault slip models of the 2010-2011 Canterbury, New Zealand, earthquakes from geodetic data and observations of postseismic ground deformation. New Zealand Journal of Geology and Geophysics, **55**(3), 207-221.

Bradley, B.A. 2012. Strong ground motion characteristics observed in the 4 September 2010 Darfield, New Zealand earthquake. *Soil Dynamics and Earthquake Engineering*, **42**, 32-46.

Bradley, B.A. 2013. Systematic ground motion observations in the Canterbury earthquakes and region-specific non-ergodic empirical ground motion modeling, *Earthq. Spectra*, 131230112032001, doi:10.1193/053013EQS137M.

Bradley, B.A., & Cubrinovski, M. 2011. Near-source Strong Ground Motions Observed in the 22 February 2011 Christchurch Earthquake, *Seismol. Res. Lett.*, **82**, 853–865, doi:10.1785/gssrl.82.6.853.

Brown, L.J., Reay, M.B. & Weeber, J.H. 1992. *Geology of the Christchurch urban area*, Institute of Geological and Nuclear Sciences.

Fry, B., Benites, R.A., Kaiser, A.E. 2011 The character of accelerations in the Mw 6.2 Christchurch Earthquake. *Seismological Research Letters*, **82**(6): 846-852; doi: 10.1785/gssrl.82.6.846

Gelagoti, F., Kourkoulis, R., Tsirantonaki, D., Gazetas, G. 2014. 2-Dimensional non-linear valley efects at Heathcote Valley during the 2011 Canterbury earthquake: A case study, *Second European Conference on Earthquake Engineering and Seismology*, Istanbul Aug. 25-29, 2014

Johnson, D.H., & Dudgeon, D.E. 1992. *Array signal processing: concepts and techniques*, Simon & Schuster.

Kawase, H. 1996. The cause of the damage belt in Kobe:"The basin-edge effect," constructive interference of the direct S-wave with the basin-induced diffracted/Rayleigh waves, *Seismol. Res. Lett.*, **67**(5), 25–34.

Konno, K., & Ohmachi, T. 1998. Ground-motion characteristics estimated from spectral ratio between horizontal and vertical components of microtremor, *Bull. Seismol. Soc. Am.*, **88**(1), 228–241.

Kuhlemeyer, R.L., & Lysmer, J. 1973. Finite element method accuracy for wave propagation problems, *J. Soil Mech. & Found. Div*, **99**(Tech Rpt).

Matheron, G. 1963. Principles of geostatistics, *Econ. Geol.*, **58**(8), 1246–1266.

Mazzoni, S., McKenna, F., Scott, M.H., & Fenves, G.L. 2007. OpenSees Command Language Manual. Pacific Earthquake Engineering Research Center, *Univ. California, Berkeley*.

Park, C.B., Miller, R.D., & Xia, J. 1999. Multichannel analysis of surface waves, *Geophysics*, **64**(3), 800–808, doi:10.1190/1.1444590.

Wathelet, M. 2005. GEOPSY Geophysical Signal Database for Noise Array Processing, *Software, LGIT, Grenoble, Fr.*

Wood, C.M., Cox, B.R., Wotherspoon, L.M., & Green, R.A. 2011. Dynamic site characterization of Christchurch strong motion stations, *Bull. New Zeal. Soc. Earthq. Eng.*, **44**(4), 195–204.